Journal of Interventional Medicine 3 (2020) 83–88

HOSTED BY

Contents lists available at ScienceDirect

Journal of Interventional Medicine

journal homepage: www.keaipublishing.com/cn/journals/journal-of-interventional-medicine/

Evaluate the characteristics and clinical significance of "toxic twin-leaf" sign in spinal epidural metastases before percutaneous vertebroplasty

Xiqi Sun, Qinghua Tian, Chungen Wu *, Yongde Cheng

Department of Diagnostic and Interventional Radiology, Shanghai Sixth People's Hospital East Affiliated to Shanghai University of Medicine & Health Sciences, Shanghai, 201316, China

ARTICLE INFO

Keywords:
"Toxic twin-leaf" sign
Magnetic resonance imaging
Spinal metastasis

ABSTRACT

Objective: Our study aimed to analyze morphological features of spinal epidural metastases using magnetic resonance imaging (MRI) and investigate the formation mechanism and clinical significance of the "toxic twin-leaf" sign in spinal epidural metastasis.

Materials and methods: We retrospectively studied 108 patients with spinal epidural metastases who underwent MRI. Patients were divided into "toxic twin-leaf" sign group (group A) and irregular group (group B). Chi-square test was used to analyze data on sex, vertebra location, presence of fracture in the corresponding vertebral body, involvement of the corresponding pedicle, and the primary tumor. Further, group data were analyzed using the rank sum test; $p < 0.05$ was considered significant.

Results: The "twin-leaf" sign was noted in 88 cases with 136 epidural masses and 20 cases of irregular shape in 108 patients; the "toxic twin-leaf" sign accounted for 87.18% of spinal epidural metastases. A difference between groups in the vertebra location ($p < 0.01$) was observed, but no differences were found in sex, presence of fractures in the corresponding vertebral body, involvement of the corresponding pedicle, and primary tumor ($p > 0.05$). Intergroup differences in the rate of spinal stenosis on axial and sagittal images were significant.

Conclusions: MRI axial sequences clearly revealed the morphology of spinal epidural metastases. Detection of the "toxic twin-leaf" sign in spinal epidural metastases was of great clinical significance. Furthermore, determining the degree of spinal stenosis in the axial sequence provided a more accurate evaluation of patients' condition compared to the sagittal sequence.

Introduction

Spinal metastasis is a common cause of thoracolumbar back pain and is involved in approximately 40% of the patients who die of cancer.[1–4] When the lesion stimulates the periosteum or accompanies a pathological fracture, it produces obvious intractable pain, which seriously affects patients' quality of life. When soft tissue masses in the spinal epidural space cause spinal canal stenosis, timely treatment is important. In early stages of spinal cord compression, symptoms are generally not evident, resulting in inadequate clinical attention. Furthermore, once symptoms appear, most doctors rely on magnetic resonance imaging (MRI) sagittal sequences to determine the degree of spinal stenosis and often underestimate patient condition, leading to lack of timely treatment, which in turn causes irreversible spinal cord injury. Therefore, early recognition of spinal canal stenosis and correct judgment of the stenosis degree are critical for appropriate treatment. As an important means of diagnosing multiple spinal metastases, MRI is becoming a common method for the detection and diagnosis of spinal metastases. Most researchers in this field have a thorough understanding of the nature, blood supply, and metabolism of soft tissue masses, but only few have analyzed the morphological characteristics of intraspinal metastases and the corresponding degree of spinal stenosis on MRI. Therefore, in this study, we retrospectively studied the morphological characteristics of intraspinal metastases on MRI axial sequences, determined stenosis rates using axial and sagittal images, and analyzed the clinical significance of the "toxic twin-leaf" sign in spinal metastases.

Materials and methods

Ethical approval

The study was approved by the ethics committee of Shanghai Sixth

* Corresponding author. Department of Diagnostic and Interventional Radiology, Shanghai Sixth People's Hospital East Affiliated to Shanghai University of Medicine & Health Sciences, China.

E-mail address: wucgsh@163.com (C. Wu).

https://doi.org/10.1016/j.jimed.2020.03.005

Available online 30 March 2020

People's Hospital East Affiliated to Shanghai University of Medicine & Health Sciences. All clinical practices and observations were conducted in accordance with the Declaration of Helsinki. Informed consent was obtained from each patient before the study was conducted.

Study population

We retrospectively reviewed 108 cases of intraspinal metastases diagnosed in our hospital from January 2016 to October 2018. The following basic information was recorded for each patient: age (years), course (months), sex (cases), involved vertebral bodies (number), location of spinal metastases (number), single or multiple vertebra (cases), involved vertebral pedicle (number), vertebrae with pathological fractures (number), total spinal epidural masses (number), "toxic twin-leaf" epidural masses (number), and history of primary tumors. The study included 78 men and 30 women with an average age of 58.53 years and disease course between 0.5 and 60 months. Primary lesion was lung cancer, liver cancer, renal cancer, pancreatic cancer, cervical cancer, prostate cancer, gastrointestinal cancer, and others in 45, 21, 10, 7, 7, 7, 6, and 5 cases, respectively (Tables 1 and 2).

Scanning equipment and methods

MRI was performed with a 1.5T superconducting MR scanner (United Imaging Healthcare) using standard surface coils for the cervical, thoracic, and lumbar spinal regions. All images were obtained using multi-slice spin echo sequences–sagittal, coronal, and axial T2-weighted sequences; sagittal T1-weighted sequence; and sagittal and axial T1-weighted enhanced sequences.

Determination of the spinal stenosis rate

The spinal stenosis rate of intraspinal metastases was determined using the median sagittal sequence and axial T2-weighted images. It was equal to the maximum transverse diameter at the level of the mass/normal transverse diameter of the vertebral canal above the mass in the median sagittal T2-weighted images, while in the axial T2-weighted images, it was equal to the maximum area of the mass divided by the normal spinal canal area above the mass.

Outcome measures and statistical analysis

SPSS20.0 statistical software was used to analyze statistical data. Data are expressed as mean ± standard deviation (x ± s). The rank sum test was used for intragroup comparison, while the chi-square test was used for counting data (χ^2 test). Differences were statistically significant when $p < 0.05$.

Results

MR images from 108 patients with spinal epidural metastases showed that 475 vertebral bodies were involved. The highest number of cases showed lumbar intraspinal metastases (8, 49, and 51 cases of cervical, thoracic, and lumbar vertebra involvement). Multiple vertebrae were mostly involved; we identified 21 cases with solitary vertebral body involvement and 87 cases with multiple vertebra involvement (consecutive pattern: 40 cases; skip pattern: 47 cases). No intervertebral disc involvement was found. Vertebral pedicle involvement was noted in 118 cases. There were 126 pathological fractures in the involved vertebrae, while there were 111 pathological fractures in the corresponding vertebrae with intraspinal metastases, which appeared as wedge-shaped, inverted wedge-shaped, and fish-like changes on MRI of the vertebrae (Table 1).

Vertebral signals of spinal metastases appeared as patchy, large patchy hypointensity, or slight hypointensity on T1-weighted images and as hypointensity, equal intensity, and hyperintensity on T2-weighted images. Some lesions appeared uneven, and lesions showed different degrees of enhancement. Signal characteristics of spinal epidural masses were as follows: hypointensity or slight hypointensity on T1-weighted images and hyperintensity on T2-weighted images; asymmetric enhancement was found after enhancement (Figs. 1 and 2). All spinal epidural metastases occurred in the ventral epidural space and only at the vertebral level. No intervertebral disc was involved. Morphological characteristics of spinal epidural metastases and stenosis of spinal canal were better revealed with contrast-enhanced T1-weighted axial and T2-weighted axial imaging than sagittal imaging (Figs. 1 and 2). 88 cases of spinal epidural metastases were of the "toxic twin-leaf" type and 20 were irregular. There were 136 masses with the "toxic twin-leaf" sign, with the following specific distribution: The number of epidural metastases occurring at the C5 and T1–L5 vertebral levels was respectively 1, 1,

Table 1
Basic information of patients with spinal metastases.

Parameter	Data
Age (years,x ± s)	58.53 ± 14.78(2085)
Course (months)	(0.5 ~ 60)
Male/female (cases)	78/30
Involved vertebral bodies (number)	475
Cervical/thoracic/lumbar vertebrae (number)	8/68/80
Single/multiple vertebrae (cases)	21/87
Involved vertebral pedicle (number)	118
Vertebrae with pathological fractures (number)	126
"Toxic twin-leaf" sign/spinal epidural masses (number)	136/156(87.18%)

Table 2
Comparison of intraspinal metastases.

Parameter	"Toxic twin-leaf" sign (group A)	Irregular shape (group B)	χ^2 value	*p value*
Sex (cases)			0.740	0.390
Male	62	16		
Female	26	4		
Vertebrae (number)			42.228	<0.001
Cervical	1	7		
Thoracic	65	3		
Lumbar	70	10		
Corresponding pedicle Involvement (number)			3.046	0.081
No	30	8		
Yes	106	12		
Corresponding vertebrae with pathological fracture (number)			0.492	0.483
No	25	5		
Yes	111	15		
Primary tumor (cases)			2.060	0.956
Liver cancer	18	3		
Lung cancer	37	8		
Renal cancer	8	2		
Pancreatic cancer	6	1		
Cervical cancer	5	2		
Prostatic cancer	6	1		
Gastrointestinal neoplasms	4	2		
Other tumors	4	1		

Table 3
Statistics of spinal stenosis rates.

Parameter	"Toxic twin-leaf" sign (group A)	Irregular shape (group B)
Spinal stenosis rates in axial T2-weighted image (x ± s)	38.97 ± 19.454	35.70 ± 19.034
Spinal stenosis rates in sagittal T2-weighted image (x ± s)	14.62 ± 18.675	35.10 ± 21.054
Z value	−9.556	−1.811
p value	<0.001	0.070

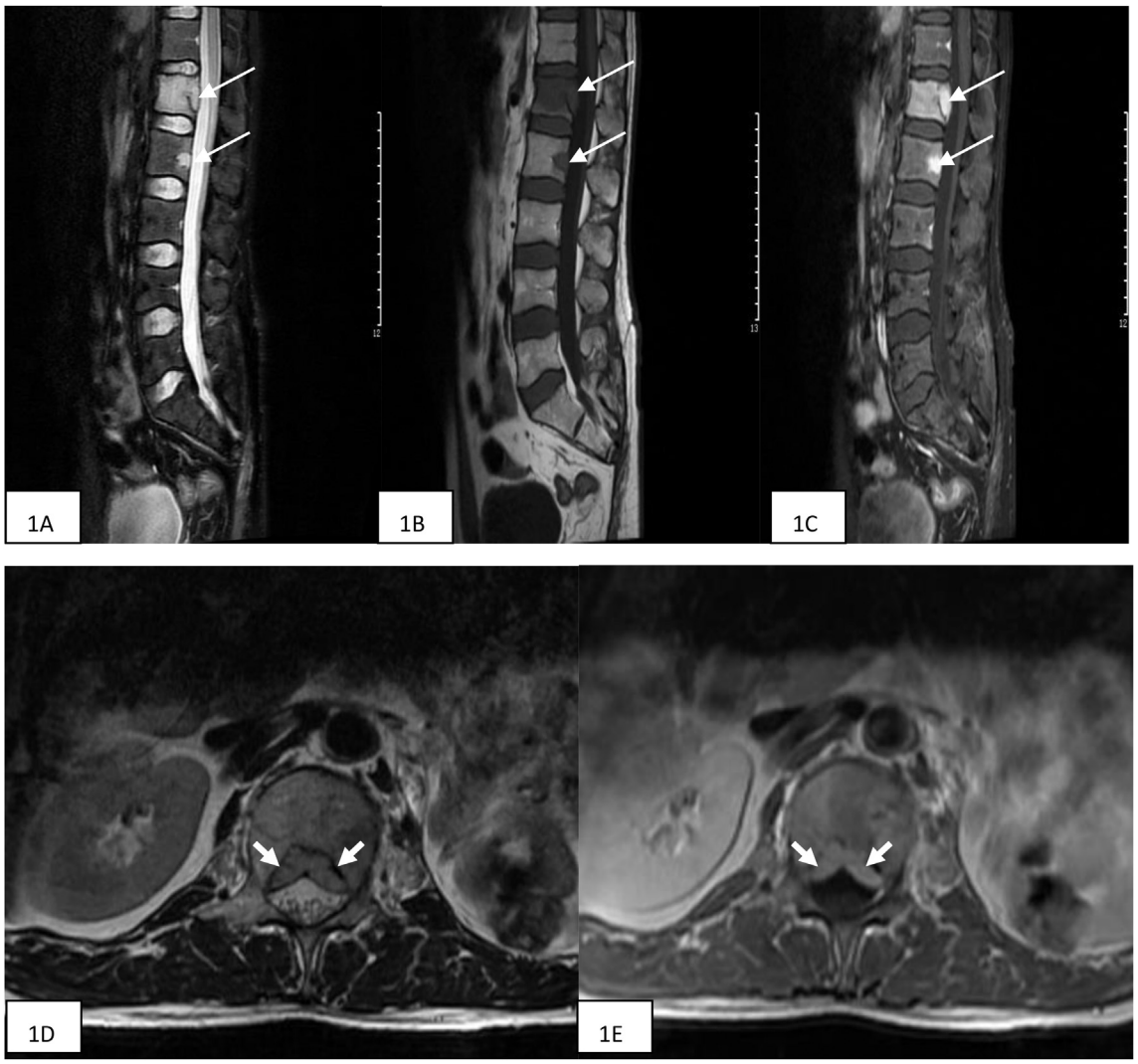

Fig 1. MRI of Spinal Epidural Metastases 1 ("Toxic twin-leaf" sign) 1A-1E. Fat-suppressed T2-weighted median sagittal image showing L1 and L2 with hyperintense metastatic bone marrow lesions and homogeneous signal intensity of lesions (1A). T1-weighted median sagittal image showing hypointensity of lesions (1B) and fat-suppressed contrast-enhanced T1-weighted median sagittal image showing heterogeneous enhancement (1C). No significant stenosis of the corresponding spinal canal is found in the fat-suppressed T2-weighted sagittal image, in the fat-suppressed contrast-enhanced T1-weighted median sagittal image (1A) and in the contrast-enhanced T1-weighted median sagittal image (1C) (Underestimation of patient's condition). T2-weighted axial image showing that L1 presents with a slightly hyperintense metastatic bone marrow lesion and a slightly hyperintense soft tissue mass in the epidural space of the spinal canal, which appears as a "twin leaf" (1D). Contrast-enhanced T1-weighted axial image showing that L1 presents with heterogeneous enhancement, while soft tissue mass presents with homogeneous enhancement (1E). Mild stenosis of the corresponding spinal canal is found in the T2-weighted axial image and contrast-enhanced T1-weighted axial image (1D and 1E).

5, 5, 4, 8, 6, 7, 7, 4, 6, 4, 8, 27, 15, 15, 9, 4 (Figure 3). In most patients, a varying degree of stenosis of the spinal canal was observed.

We found an intergroup significant difference in the location of the vertebral metastasis ($p < 0.01$), based on the chi-square test of spinal epidural masses. There were no significant intergroup differences in sex, corresponding pedicle involvement, corresponding vertebrae with pathological fractures, and primary tumor ($p = 0.390$, 0.081, 0.483, and 0.956, respectively).

We carefully analyzed the MR images and then determined the stenosis rates of spinal epidural metastases in groups A and B on the axial and sagittal T2-weighted images. For group A, the mean spinal stenosis rates in the axial and sagittal T2-weighted images were 38.97 ± 19.454 and 14.62 ± 18.675, respectively. The results of the rank sum test (Z value) for spinal stenosis rates were -9.556 ($p < 0.01$). There was a significant difference in spinal stenosis rates between the axial and sagittal T2-weighted images in group A. Further, axial T2-weighted images afforded a better evaluation of spinal stenosis rate than sagittal images. For group B, the mean and standard deviations determined using axial and sagittal T2-weighted images were 35.70 ± 19.034 and 35.10 ± 21.054, respectively. The results of the rank sum test (Z value) of spinal stenosis rates were -1.811 ($p = 0.070$) (Table 3). There was no significant intergroup difference, indicating that there was no significant difference in the spinal stenosis rates between the axial and sagittal T2-weighted images.

Discussion

Characteristics of spinal metastases

Spinal metastasis, followed by lung and liver metastasis, is a common complication of malignant neoplasms.[5,6] Epidural metastasis is also common and appears as the initial manifestation of cancer in approximately 20% of all cases of spinal epidural metastases.[7,8] Unalleviated pain is a common symptom.[9–12]

Spinal metastases occur mostly through blood, primarily because the vertebrae mostly consist of cancellous bone and contain relatively rich blood circulation; in addition, because of the barrier imposed by the

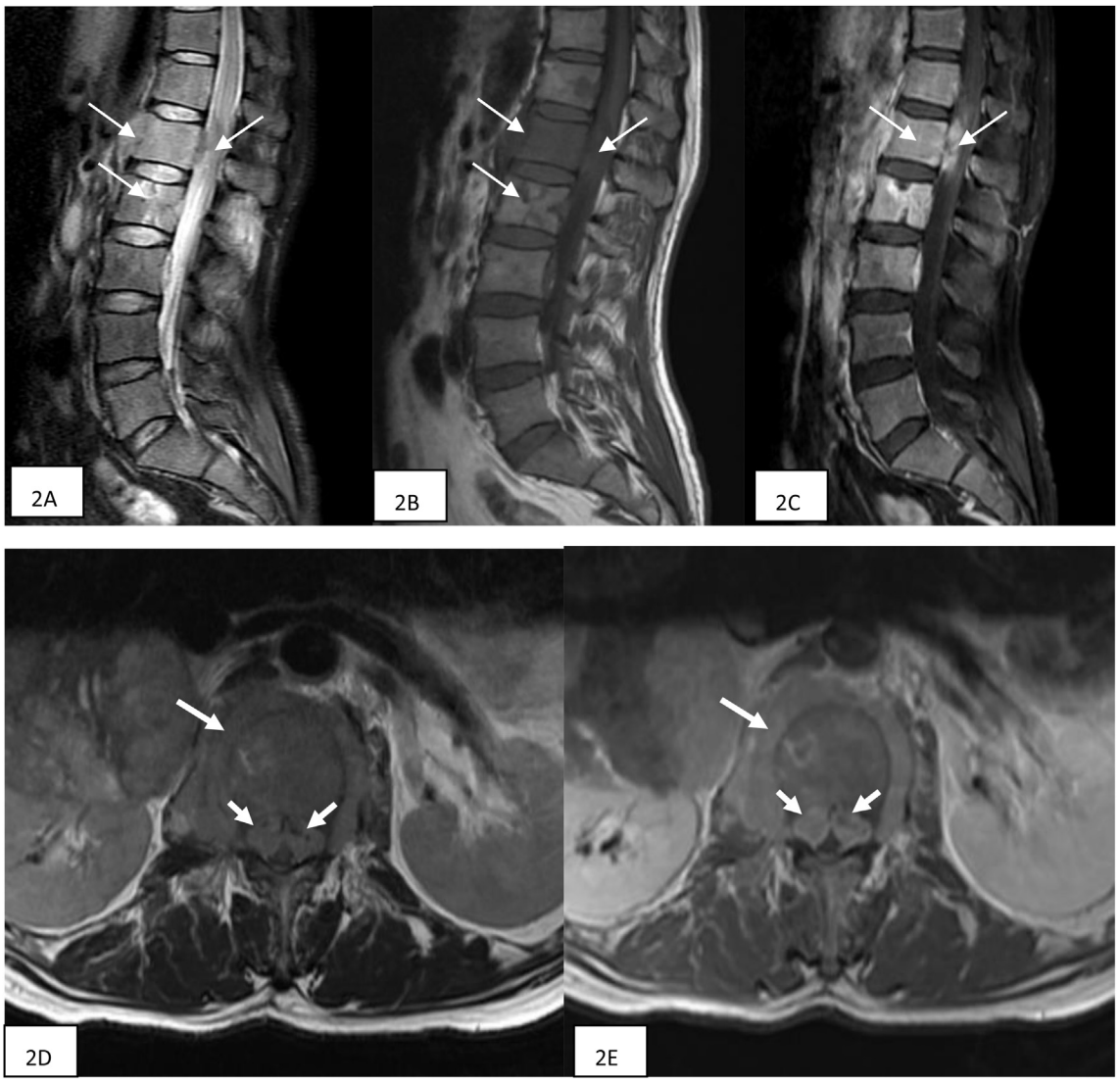

Fig 2. MRI of Spinal Epidural Metastases 2 ("Toxic twin-leaf" sign) 2A-2E. Fat-suppressed T2-weighted median sagittal image (2A), T1-weighted median sagittal image (2B), fat-suppressed contrast-enhanced T1-weighted median sagittal image (2C) showing that L1-2 present with hyperintense metastatic bone marrow lesions in the T2-weighted image, hypointensity on the T1-weighted image, and heterogeneous enhancement. Signal characteristics of prevertebral and epidural masses are similar to those of vertebral lesions. Moderate stenosis of the corresponding spinal canal is found in the median sagittal image (2A-2C) (Underestimation of patient's condition). T2-weighted axial image (2D), contrast-enhanced T1-weighted axial image (2E) showing that L1, prevertebral and epidural masses present with slight hyperintensity on the T2-weighted image and obvious enhancement; epidural masses appear as the "twin-leaf" sign. Severe stenosis of the corresponding spinal canal is found in the axial image (2D and 2E).

periosteum, it is difficult for some non-invasive tumors to directly invade the contiguous vertebral body. The capillary network of the red bone marrow in the vertebral body is suitable for the growth of tumors. After the tumors enter the vertebral body, they first infiltrate the fat cells of the bone marrow, followed by involvements of the cortex and appendages of the bone. Malignant tumors are usually disseminated through the spinal venous system. The posterior part of the vertebral body is the first site of spinal metastasis, which is consistent with the entry site of the vertebral blood vessels. Spinal metastases frequently involve the pedicle because of its unique structure, which consists of relatively thick cortex surrounding cancellous bone and is easy to identify on plain radiography.

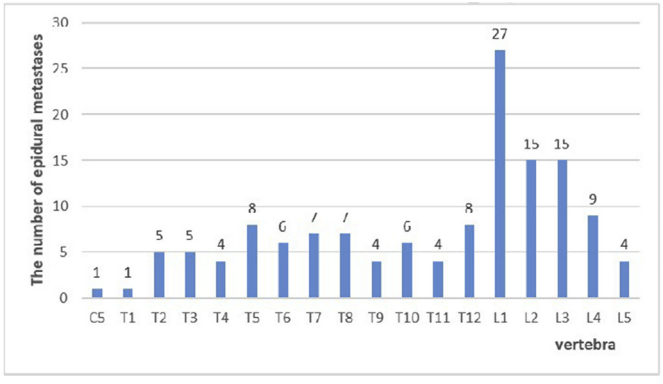

Fig 3. Vertebra with "toxic twin-leaf" sign of the epidural metastases.

In comparison with other spinal diseases, spinal metastases often show jumping distribution. These metastases can be classified as showing osteogenic, osteolytic, or mixed bone destruction. Most metastatic tumors show osteolytic destruction, while a few show the osteogenic pattern. The primary tumors that are prone to osteogenic metastasis are prostate cancer, osteosarcoma. Among radiography, CT and MRI, MRI shows the highest sensitivity and specificity for the diagnosis of spinal metastases. In MR images, normal bone marrow shows a higher signal on T1WI sequences, while the bone marrow signal associated with

metastatic lesions is lower, leading to an uneven signal. Thus, T1-weighted images are sensitive for the detection of lesions. The signal in T2-weighted images is different, and these images can show high, low, and mixed signals. After enhancement, lesions appear homogeneous with uneven enhancement.[13,14]

Nomenclature of the "toxic twin-leaf" sign in spinal epidural metastasis

The "toxic twin-leaf" sign refers to the linear intact cortical area in the central area (posterior vertebral body) of the vertebrae without obvious soft tissue mass, while the symmetrical soft tissue mass in the para-vertebral central area (both lateral posterior vertebrae) that forms an octagonal shape is a "twin-leaf" sign. This sign usually appears during compression and injury of the spinal cord and is caused by the bilateral space-occupying effect of a soft tissue mass, which is significantly higher than that of a unilateral mass. The "twin-leaf" sign is easy to cause abolishment of sensory and motor functions, even paraplegia, below the corresponding vertebral plane. When metastatic tumors in the spinal canal show this sign, the spinal canal stenosis rate is often higher in the axial image than in the sagittal image. However, most experts judge the degree of spinal stenosis on the basis of sagittal images; therefore, the severity of the condition is often underestimated. In addition, spinal metastasis progresses very quickly and is very aggressive. If it is not controlled on time, it will have a substantial impact on the prognosis of patients. Therefore, in order to emphasize the harmful effects associated with this phenotype, we named it the "toxic twin-leaf" sign.

MRI provides high-resolution images of soft tissue and can appropriately display soft tissue morphology along with signal characteristics and invasion of surrounding tissues. In particular, the shape of spinal epidural metastasis is very well visualized in axial T2-weighted images. Some authors have described intraspinal metastasis using a typical "double-bag" configuration with T1-weighted imaging,[6] which may represent another description of the "toxic twin-leaf" sign. Although many reports have described the formation of spinal metastasis with a soft tissue mass in the spinal canal, there is no definite report on the formation of the "toxic twin-leaf" sign in the spinal canal. Our study attempts to analyze the anatomical factors associated with this sign.

Mechanism of the formation of the "toxic twin-leaf" sign in spinal epidural metastases

Because of the rich venous plexus in the extramedullary epidural space of the spinal canal, venous plexus is composed of a "lake" venous network without valves and a relatively slow blood flow. Cancer cells can easily enter the vertebral body through the venous plexus, and therefore, metastatic tumors of the spinal vertebral body mostly occur in the posterior part of the vertebrae. Because the anterior venous plexus in the spinal canal is distributed in the medial part of the pedicle, the main vascular plexus is in the medial part of the pedicle and shows a wide range and diameter.[15] Therefore, vertebral metastases often involve the pedicle.

There were 136 "twin-leaf" masses and 20 irregularly shaped masses in 108 patients with spinal epidural metastases, which may be mainly related to the posterior longitudinal ligament in the posterior margin of the vertebrae. The posterior longitudinal ligament is a banded fiber located at the anterior edge of the anterior epidural space extended along the posterior surfaces of the bodies of the vertebrae. It originates from the foramen magnum of the occipital bone, passing through the tectorial membrane, to the sacrum. These ligaments attach to the posterior edge of the vertebrae and to the posterior edge of the intervertebral disc. Their main function is to maintain the normal tension of the vertebral body. Horizontally, at the upper margin of the vertebrae, the central portion of the posterior longitudinal ligament is composed of a three-layer fibrous structure, which extends vertically and longitudinally. The structure is compact and orderly, with no loose connective tissue filling. In contrast, in the posterolateral part of the vertebrae, that is, the paracentral paravertebral area, the ligament is composed of two layers of fibers, no middle layer of fibrous covering, an oblique walking direction, more relaxed structure, disordered arrangement, and a large amount of loose connective tissue filling. These factors lead to a relatively weaker area in the para-canal central area than in the central area of the vertebrae. Cancer cells are prone to invade the weak area of the vertebrae and form a "toxic twin-leaf" sign.

The tightness of the posterior longitudinal ligament at the level of the vertebral body and intervertebral disc is different. At the vertebral level, the ligament is not completely attached to the vertebrae and is loosely connected with the posterior edge of the vertebrae. The deep dentate fibers can be seen by simple dissection. In contrast, at the level of the intervertebral disc, the ligament covers the posterior edge of the disc and connects closely with the annulus fibrosus of the intervertebral disc, extending to the intervertebral foramen posteriorly on both sides.[16] Moreover, the posterior longitudinal ligament is narrower at the level of the vertebrae than at the intervertebral disc. These factors may be related to the formation of the "toxic twin-leaf" sign at the level of the vertebrae rather than at the intervertebral disc. The cervical spine has uncinate joints at the level of the intervertebral disc, which reduces the likelihood of metastasis of the vertebrae at the level of the intervertebral disc. In general, a significant difference in the length of the posterior longitudinal ligament was not found in the right-left and male-female comparisons.[17]

Table 2 shows that the intraspinal metastases in group A included 1 mass in the cervical vertebrae, 65 masses in the thoracic vertebrae, and 70 masses in the lumbar vertebrae, while there were 7 masses in the cervical vertebrae, 3 masses in the thoracic vertebrae, and 10 masses in the lumbar vertebrae in group B. The results of the chi-square test for spinal epidural masses in groups A and B showed a significant difference in the location of vertebral metastases between the two groups. In this statistical assessment, cervical metastasis showed the lowest frequency and mostly occurred in the thoracic and lumbar vertebrae, which may be related to patient's primary tumors. Some investigators have suggested that the location of spinal metastases may differ between patients with different primary tumors, which may be related to the vertebral blood supply and venous drainage. For example, thyroid cancer may easily metastasize to the cervical vertebrae, lung cancer to the thoracic vertebrae, and liver cancer, uterine malignant tumors, and prostate cancer, may easily metastasize to the lumbosacral vertebrae.[18] The primary tumors in this study were mostly located in the chest, abdomen, and pelvis. Therefore, the spinal metastases were mostly found on the thoracic and lumbar vertebrae, which was consistent with the above findings. In this case, the highest proportion of "toxic twin-leaf" sign metastases occurred at the thoracic vertebral level, which may be related to the shape and thickness of the posterior longitudinal ligament. The central part of the posterior longitudinal ligament is narrower and slightly thicker at the thoracic level than at the other vertebral levels. Therefore, thoracic epidural metastases are more likely to form the "twin-leaf" sign than other vertebrae. In the lumbar region, the thick central portion appears to decrease in width from L1 to L5.[19] In addition, Hofmann's ligaments are fibrous bands of connective tissue on the anterior spinal epidural space that connect the anterior dural sac to the posterior longitudinal ligament.[20,21] These ligaments were "thicker and better developed" in the lower lumbar vertebrae than in the upper lumbar regions in previous studies,[22] which may lead to a looser connection of the posterior longitudinal ligament in the lower lumbar spine than in the upper lumbar spine. Therefore, spinal epidural metastases in the lower lumbar spinal canal are more irregular than those in the upper lumbar spinal canal.

Correct understanding of the clinical significance of the "toxic twin-leaf "sign

Our statistical assessment showed a significant difference in spinal canal stenosis rates between the axial and sagittal T2-weighted images in group A. The spinal canal stenosis rate was significantly higher in axial T2-weighted images than in sagittal images. However, there was no

significant difference in the spinal canal stenosis rate between the axial and sagittal T2-weighted images in group B. Therefore, for the "toxic twin-leaf" spinal epidural metastasis, it was more accurate to assess the spinal stenosis rate and patient's condition in the axial T2-weighted image than in the sagittal image.

Early spine metastasis only causes vertebral signal abnormality in MRI, and clinical symptoms may not be obvious or manifest only as neck body, chest, and back pain. Vertebral pathological fracture, soft tissue mass, and spinal canal involvement may appear subsequently. When spinal metastases present with pathological fractures or lesions involving the dural sac, they can cause intolerable radiation pain in the neck and back. When accompanied by spinal stenosis, they can also lead to serious complications such as limb numbness, weakness, dyskinesia, and limps. Without early control, these patients may experience irreversible spinal cord injury, resulting in loss of motor and sensory functions below the pathological level, incontinence of stool and urine, and inability to take care of themselves.[23] Therefore, for patients with spinal metastases, it is necessary to identify the "toxic twin-leaf" sign in axial T2-weighted images and contrast-enhanced T1-weighted images as early as possible and to correctly evaluate the spinal canal stenosis rate. This can allow early interventions for disease progression and alleviate spinal cord injury; additionally, this approach can also be used to guide interventional treatment. When the spinal canal is obviously narrow, it can be removed first, which can be followed by interventional treatment such as percutaneous vertebroplasty, I^{125} implantation or radiofrequency ablation. When the spinal canal is severely narrowed or the patient presents with severe spinal cord injury symptoms, radiotherapy or targeted drug therapy can be selected, thereby avoiding ineffective treatment.

In conclusion, detection of the "toxic twin-leaf" sign in spinal epidural metastases is of great clinical significance. Measurements of the spinal canal stenosis rate are more accurate in axial T2-weighted images than in sagittal images, and these measurements are critical for guiding clinical treatment and the choice of treatment methods.

Patient consent

Witten informed consent was obtained from patients for publication of these case reports and any accompanying images.

Declaration of interests

The authors declare that they have no known competing financial interests or personal relationships that could have appeared to influence the work reported in this paper.

References

1. Araujo JL, Veiga JC, Figueiredo EG, et al. Management of metastatic spinal column neoplasms - an update. *Rev Col Bras Cir*. 2013;40:508–514.
2. Husain ZA, Sahgal A, Chang EL, et al. Modern approaches to the management of metastatic epidural spinal cord compression. *CNS Oncol*. 2017;6:231–241.
3. Daniel JW, Veiga JC. Prognostic parameters and spinal metastases: a research study. *PloS One*. 2014;9, e109579.
4. Oliveira MF, Barros Bde A, Rotta JM, et al. Tokuhashi Scoring System has limited applicability in the majority of patients with spinal cord compression secondary to vertebral metastasis. *Arq Neuropsiquiatr*. 2013;71:798–801.
5. Wu LM, Gu HY, Zheng J, et al. Diagnostic value of whole-body magnetic resonance imaging for bone metastases: a systematic review and meta-analysis. *J Magn Reson Imag*. 2011;34:128–135.
6. Guzik G. Current incidence of different morphological types of malignant metastases to the spine based on magnetic resonance imaging. *Ortop Traumatol Rehabil*. 2017;19:137–144.
7. Jacobs WB, Perrin RG. Evaluation and treatment of spinal metastases: an overview. *Neurosurg Focus*. 2001;11:e10.
8. Liu WM, Xing R, Bian C, et al. Predictive value of pedicle involvement with MRI in spine metastases. *Oncotarget*. 2016;7:62697–62705.
9. Choi D, Crockard A, Bunger C, et al. Review of metastatic spine tumour classification and indications for surgery: the consensus statement of the Global Spine Tumour Study Group. *Eur Spine J*. 2010;19:215–222.
10. Mut M, Schiff D, Shaffrey ME. Metastases to the nervous system: spinal epidural and intramedullary metastases. *J Neuro Oncol*. 2005;75:43–56.
11. Ejima Y, Matsuo Y, Sasaki R. The current status and future of radiotherapy for spinal bone metastases. *J Orthop Sci*. 2015;20:585–592.
12. Lee CH, Kwon JW, Lee J, et al. Direct decompressive surgery followed by radiotherapy versus radiotherapy alone for metastatic epidural spinal cord compression: a meta-analysis. *Spine*. 2014;39:E587–E592 (Phila Pa 1976).
13. Lang N, Su MY, Yu HJ, et al. Differentiation of tuberculosis and metastatic cancer in the spine using dynamic contrast-enhanced MRI. *Eur Spine J*. 2015;24:1729–1737.
14. Mittal S, Khalid M, Sabir AB, et al. Comparison of magnetic resonance imaging findings between pathologically proven cases of atypical tubercular spine and tumour metastasis: a retrospective study in 40 patients. *Asian Spine J*. 2016;10:734–744.
15. Pan L, Li ZH, Ma LT. Study of applied anatomy of in-travertebral venous plexuy. *Chinese Journal of Clinical Neuro-surgery*. 2006;11:664–666.
16. Prestar FJ. Morphology and function of the interspinal ligaments and the supraspinal ligament of the lumbar portion of the spine. *Morphol Med*. 1982;2:53–58.
17. Lee SB, Chang JC, Lee GS, et al. Morphometric study of the lumbar posterior longitudinal ligament. *J Korean Neurosurg Soc*. 2018;61:89–96.
18. Bhattacharya IS, Hoskin PJ. Stereotactic body radiotherapy for spinal and bone metastases. *Clin Oncol (R Coll Radiol)*. 2015;27:298–306.
19. Ohshima H, Hirano N, Osada R, et al. Morphologic variation of lumbar posterior longitudinal ligament and the modality of disc herniation. *Spine (Phila Pa 1976)*. 1993;18:2408–2411.
20. Wiltse LL. Anatomy of the extradural compartments of the lumbar spinal canal. Peridural membrane and circumneural sheath. *Radiol Clin*. 2000;38:1177–1206.
21. Tardieu GG, Fisahn C, Loukas M, et al. The epidural ligaments (of Hofmann): a comprehensive review of the literature. *Cureus*. 2016;8:e779.
22. Wadhwani S, Loughenbury P, Soames R. The anterior dural (Hofmann) ligaments. *Spine (Phila Pa 1976)*. 2004;29:623–627.
23. Lang N, Su MY, Yu HJ, et al. Differentiation of tuberculosis and metastatic cancer in the spine using dynamic contrast-enhanced MRI. *Eur Spine J*. 2015;24:1729–1737.